Available online at www.sciencedirect.com
SCIENCE DIRECT®
Journal of Chromatography A, 1018 (2003) 213–223
JOURNAL OF CHROMATOGRAPHY A
www.elsevier.com/locate/chroma

Experimental determination of adsorption energies, adsorption isotherms, probability density functions, and lateral molecular interactions on C_XH_Y/CaO systems

S. Margariti, V. Siokos, F. Roubani-Kalantzopoulou*

School of Chemical Engineering, National Technical University of Athens, 15780 Zografou, Athens, Greece

Received 9 May 2003; received in revised form 29 July 2003; accepted 8 August 2003

Abstract

Reversed-flow gas chromatography (RF-GC) is extended to the measurements of the probability density function for the adsorption energies as well as the differential energies of adsorption due to lateral interactions of molecules adsorbed on different heterogeneous solid surfaces. All these calculations are based on a non-linear adsorption isotherm model as it is well accepted that the linear one is inadequate for substances such as these used in this work. Thus, some new important physicochemical parameters have been obtained for the characterization of the heterogeneous systems studied. The adsorbent used in this study was calcium oxide. The adsorption of many significant hydrocarbons was investigated. With these systematic experiments under conditions which are similar to the atmospheric ones, an extrapolation of the results obtained to "real" atmospheres with a high degree of confidence is possible.

Keywords: Gas chromatography, reversed-flow; Inverse gas chromatography; Probability density functions; Molecular interactions; Adsorption isotherms; Adsorption energies

1. Introduction

When adsorption takes place at finite surface coverages, the isotherms are generally non-linear and hence, retention volumes in gas chromatography are dependent upon the adsorbate concentration in the gas phase. In addition, a non-linear isotherm results in asymmetrical peaks, the shape of which and the retention time are dependent on the volume injected.

In a previous work [1], it was mentioned that the majority of papers devoted to single-gas adsorption assumed that the surface of the adsorbent is homogeneous [2–5]. However, single-gas adsorption systems with adsorbate molecules of complex chemical structure, and adsorbents of complex chemical composition and porous structure cannot possibly be described by means of equations derived for homogeneous surfaces [5].

Reversed-flow gas chromatography (RF-GC) is a well known dynamic method combining simplicity

* Corresponding author. Tel.: +30-210-77-23-277; fax: +30-210-20-27-691.
E-mail address: roubanif@central.ntua.gr (F. Roubani-Kalantzopoulou).

0021-9673/$ – see front matter © 2003 Published by Elsevier B.V.
doi:10.1016/j.chroma.2003.08.019

with accuracy [6,7]. It is useful for measuring adsorption isotherms for complex systems where surface heterogeneity plays a very important role and must be taken into account in the physicochemical interpretation of the adsorption process [1,8–10]. This method based on two mass-balance equations, one in the gas region and the other in the solid bed one, is useful for evaluating adsorption isotherms because it gives model-independent results [11]. The RF-GC method is also described and evaluated for the determination of many physicochemical parameters based on the experimental determination of the adsorption isotherms of gas–solid systems in homogeneous gas phase [12,13] and in heterogeneous as well [14–20].

In this paper, experimental adsorption energies [21,22] are presented using the technique and the methodology of the RF-GC as well as the probability density functions [23–25] for the adsorption energies and the differential energies of adsorption due to lateral interactions [26] of C_XH_Y molecules adsorbed on CaO. Apart from that, the local monolayer capacities, the local isotherms, and the C_XH_Y equilibrium concentration are calculated and presented as a function of experimental time by a time resolved analysis [23–25].

2. Experimental

2.1. Materials

The adsorbates used were : hydrocarbons with 2–4 atoms of C, saturated or not, were obtained from Air Liquide and employed without further purification. The calcium oxide was from the Greek company S.A., 10–30 mesh and had a purity of 99%. Ultra-high-purity nitrogen was used as carrier gas.

2.2. Apparatus

Chromatographic measurements were carried out with a Shimatzu gas chromatograph, model 8A with a flame ionization detection (FID) system. The experimental arrangement was analogous to that used in [1] (cf. Fig. 1 of [1]), with some modifications. Here, the section which was empty of any solid material had a length of 22.4 cm, while that which contained the CaO solid bed was 5.2 cm. Both these sections were of Pyrex glass of 3.5 mm i.d. The sampling column of total length of 100 cm was of stainless steel chromatographic tube of 4.0 mm i.d.

2.3. Procedure

CaO was packed in the 5.2 cm solid bed. Before the adsorption experiments, this column with the adsorbent was conditioned at 473 K for 24 h under a flow of nitrogen, followed every time by the adjustment at the working temperature (323.2 K). The flow-rate measured at the outlet of the column was 26.1 $cm^3\,min^{-1}$.

A small quantity of 1 cm^3 C_XH_Y at atmospheric pressure was injected through the end of the diffusion column at atmospheric pressure, and after the appearance of the continuously rising concentration–time curve, the reversing procedure for the nitrogen carrier gas flow started and was repeated every 2 min. Each reversal lasted always 10 s, which is shorter than the gas hold-up time in the sampling column. The above procedure was done automatically by using an electronic device supplied by VICI. The narrow, fairly symmetrical sample peaks created by the flow reversals were stored in a personal computer by the CLASS VP chromatography data system, supplied by Shimadzu, and finally they were printed by an ink-jet printer.

3. Calculations

A brief outline of the theory, underlying adsorption parameters of gases on solids, is given. The calculation of all the new physicochemical parameters has been performed using recently published models [22–26].

The main equation remains Eq. (1):

$$H^{1/M} = gc(l', t) = \sum_{i=1}^{4} A_i \exp(B_i\, t) \tag{1}$$

where H is height of sample peaks resulting from the flow reversal (cm), M the response factor of the detector (dimensionless), g the calibration factor of the detector ($mol^{-1}\,cm^{-2}$), and $c(l', t)$ the measured sampling concentration of the analyte (hydrocarbon) at $x = l'$ mol cm^{-3}.

The explicit calculation of the adsorption parameters for the hydrocarbons C_2H_6, C_2H_4, C_2H_2, C_3H_6, and 1-C_4H_8 can be carried out in an analogous way

to the one described earlier [21–26]. All parameters refer to the values of $c_y(0, t)$, i.e. the concentration of the gaseous analyte C_XH_Y at $y = 0$:

$$c_y(0,t) = \frac{vL_1}{D_z} \cdot c(l',t) = \frac{vL_1}{gD_z} \cdot \sum_{i=1}^{4} A_i \exp(B_i t) \quad (2)$$

where v is the linear velocity of the carrier gas (cm s^{-1}) in the sampling column, L_1 the length of the diffusion column (cm), and D_z the diffusion coefficient of each hydrocarbon into the nitrogen carrier gas (cm^2 s^{-1}). From this, the value of the adsorbed concentration c_s^* is calculated as:

$$c_s^* = \frac{\alpha_y}{\alpha_s} k_1 \cdot \frac{vL_1}{gD_z} \cdot \sum_{i=1}^{4} \frac{A_i}{B_i} [\exp(B_i t) - 1] \quad (3)$$

where the first fraction corresponds to the ratio of the cross sectional area of the void diffusion column (cm^2) to the amount of CaO per unit length of the same column (g cm^{-1}), k_1 the local adsorption coefficient, and the rest of the symbols have been explained after Eq. (2). The local adsorption isotherm is given by:

$$\theta_t = \frac{c_s^*}{c_{\max}^*} \quad (4)$$

where $c_{\max}^*$ is the local monolayer capacity, and c_s^* is given by Eq. (3).

$$c_{\max}^* = c_s^* + \frac{\partial c_s^* / \partial c_y}{KRT} \quad (5)$$

Thus, for the $c_{\max}^*$ determination the derivative $\partial c_s^* / \partial c_y$ and KRT from Eqs. (6) and (7), respectively, are needed:

$$\frac{\partial c_s^*}{\partial c_y} = \frac{\alpha_y}{\alpha_s} \cdot k_1 \cdot \frac{\sum_{i=1}^{4} A_i \exp(B_i t)}{\sum_{i=1}^{4} A_i B_i \exp(B_i t)} \quad (6)$$

$$KRT = \frac{gD_z}{vL_1} \cdot \left\{ \frac{\sum_{i=1}^{4} A_i B_i^2 \exp(B_i t)}{\left[\sum_{i=1}^{4} A_i B_i \exp(B_i t)\right]^2} - \frac{1}{\sum_{i=1}^{4} A_i \exp(B_i t)} \right\} \quad (7)$$

In all equations above A_i and B_i are the pre-exponential factors and the exponential coefficients of Eq. (1). All the adsorption quantities mentioned have been derived and described in detail in [21–26].

The relations for calculating the adsorption energy ε (kJ mol^{-1}), the probability density function $f(\varepsilon)$, and the modified function $\varphi(\varepsilon)$ [23–25] from experimental data are given by Eqs. (8)–(10):

$$\varepsilon = RT[\ln(KRT) - \ln(RT) - \ln K^0] \quad (8)$$

$$f(\varepsilon) = \frac{\partial c_{\max}^*}{\partial \varepsilon} = \frac{\partial c_{\max}^* / \partial t}{\partial \varepsilon / \partial t} \quad (9)$$

$$\varphi(\varepsilon; t) = \frac{\theta f(\varepsilon)}{c_{\max}^*} \quad (10)$$

In [26] one can find, in an analytical way, how the differential energy of adsorption due to lateral interactions is added to adsorption energy. The starting point was again Jovanovic isotherm [5,23]. Thus, $\beta\theta$ is the added to ε differential energy of adsorption due to lateral interactions given by Eq. (11), where ω is the lateral interaction energy and z the number of neighbors for each adsorption site:

$$\beta\theta = \frac{\theta z \omega}{RT} \quad (11)$$

4. Results and discussion

Starting with the experimental values H, t of the chromatogram of any C_XH_Y/CaO system, five physicochemical quantities can be calculated by the LAT PC program [23,26] through the pre-exponential factors and the exponential coefficients of Eq. (1), namely the adsorption energy, the local adsorption isotherm, the local monolayer capacity, the energy distribution function, and the dimensionless β or ($\beta\theta$) concerning lateral interactions, all in relation to the experimental time. Table 1 shows some representative results concerning the system C_2H_6/CaO. All are tabulated with the corresponding values of c_y (in the last column). Table 2 shows standard deviations for the experimental values of A_i and B_i. On the other hand, all results concerning the heterogeneous systems studied are demonstrated in Figs. 1–4.

In Figs. 1 and 3 (part a), concerning the dependence of distribution function of adsorption energies on the adsorption energies themselves, a Gaussian curve is observed (the slight deviations from this behavior correspond to the beginning and the end of the experimental results). In Figs. 1 and 3 (part b), concerning

Table 1
Time distribution of adsorption energy, ε, local monolayer capacity, c^*_{max}, local adsorption isotherm, θ_i, energy distribution function, $\varphi(\varepsilon; t)$ lateral molecular interaction, β, and gas equilibrium concentration, c_y, for C_2H_6 on CaO at 323.2 K

t (min)	ε (kJ mol^{-1})	c^*_{max} (μmol g^{-1})	θ	$\varphi(\varepsilon; t)$ (cmol kJ^{-1}min^{-1})	β	c_y (μmol cm^{-3})
4	88.51	0.174	0.572	9.111	1.665	2.657
6	88.98	0.252	0.215	6.287	0.210	4.307
8	90.33	0.540	0.481	9.290	0.011	5.152
10	92.24	0.793	0621	8.761	−0.071	5.581
12	95.24	0.976	0.755	6.883	−0.046	5.783
14	102.7	1.065	0.927	2.503	−0.015	5.854
16	98.92	1.433	0.865	4.337	0.039	5.844
18	94.04	2.057	0.725	7.424	0.121	5.781
20	91.56	2.768	0.628	8.698	0.236	5.781
22	89.91	3.561	0.556	9.188	0.389	5.683
24	88.66	4.435	0.500	9.304	0.968	5.559
26	87.64	5.401	0.453	9.221	1.161	5.419
28	86.78	6.479	0.412	9.015	1.149	5.267
30	86.02	7.698	0.375	8.721	1.204	5.108
32	85.32	9.097	0.340	8.353	1.282	4.944
34	84.66	10.74	0.307	7.919	1.380	4.779
36	84.03	12.69	0.275	7.422	1.498	4.613
38	83.40	15.09	0.244	6.863	1.609	4.449
40	82.77	18.11	0.213	6.244	1.714	4.288
42	82.11	22.03	0.183	5.568	1.817	4.130
44	81.41	27.37	0.154	4.838	1.918	3.976
46	80.64	35.03	0.125	4.059	2.019	3.826
48	79.75	46.94	0.096	3.239	2.119	3.681
50	78.68	67.87	0.069	2.385	2.220	3.540
52	77.21	113.9	0.042	1.507	2.322	3.405
54	74.59	293.6	0.017	0.617	2.426	3.274
56	72.19	708.9	0.007	0.265	2.531	3.148
58	75.87	184.2	0.028	1.023	2.637	3.027
60	77.19	115.0	0.046	1.647	2.745	2.911
62	77.95	88.09	0.062	2.161	2.854	2.799
64	78.46	74.12	0.075	2.585	2.966	2.692
66	78.82	65.78	0.086	2.934	3.081	2.589
68	79.08	60.41	0.096	3.221	3.199	2.490
70	79.27	56.82	0.104	3.454	3.320	2.395
72	79.42	54.39	0.110	3.642	3.446	2.304
74	79.52	52.75	0.115	3.791	3.575	2.216
76	79.59	51.72	0.119	3.907	3.709	2.132
78	79.63	51.13	0.122	3.993	3.848	2.051
80	79.66	50.91	0.124	4.054	3.992	1.974
82	79.66	50.99	0.126	4.092	4.142	1.899
84	79.65	51.33	0.126	4.111	4.296	1.828
86	79.63	51.89	0.127	4.113	4.457	1.759
88	79.59	52.67	0.126	4.099	4.624	1.693
90	79.54	53.64	0.125	4.071	4.797	1.629
92	79.48	54.79	0.124	4.031	4.976	1.568
94	79.42	56.12	0.122	3.981	5.163	1.510
96	79.34	57.62	0.120	3.921	5.356	1.453
98	79.26	59.30	0.117	3.853	5.557	1.399
100	79.17	61.15	0.115	3.778	5.766	1.347
102	79.08	63.19	0.112	3.697	5.983	1.297
104	78.98	65.40	0.109	3.610	6.208	1.249

Table 1 (*Continued*)

t (min)	ε (kJ mol^{-1})	c^*_{max} (μmol g^{-1})	θ	$\varphi(\varepsilon; t)$ (cmol kJ^{-1}min^{-1})	β	c_y (μmol cm^{-3})
106	78.88	67.81	0.106	3.519	6.442	1.202
108	78.77	70.42	0.103	3.425	6.684	1.158
110	78.66	73.23	0.099	3.327	6.937	1.115
112	78.54	76.26	0.096	3.226	7.198	1.074
114	78.42	79.51	0.093	3.124	7.470	1.034
116	78.29	83.01	0.089	3.021	7.753	0.996
118	78.17	86.76	0.086	2.917	8.046	0.923
120	78.04	90.78	0.082	2.813	8.351	0.889
122	77.90	95.08	0.079	2.709	8.667	0.857
124	77.77	99.68	0.076	2.606	8.996	0.825
126	77.63	104.6	0.073	2.503	9.337	0.794
128	77.49	109.9	0.069	2.402	9.691	0.765
130	77.35	115.5	0.066	2.302	10.06	0.737
132	77.20	121.5	0.063	2.204	10.44	0.710
134	77.06	128.0	0.060	2.108	10.84	0.684
136	76.91	134.8	0.057	2.014	11.25	0.659
138	76.76	142.2	0.055	1.923	11.68	0.634
140	76.61	150.0	0.052	1.834	12.12	0.611
142	76.45	158.4	0.049	1.747	12.58	0.588
144	76.30	167.3	0.047	1.664	13.06	0.567
146	76.14	176.9	0.045	1.583	13.56	0.546
148	75.99	187.1	0.042	1.504	14.07	0.526
150	75.83	198.0	0.040	1.429	14.61	0.507

the dependence of distribution function of adsorption energies on the experimental time, one can distinguish three types of adsorption active sites. As regards (part c) in Figs. 1 and 3, a similar behavior as in case (part b) is observed.

Table 2
Standard errors of the pre-exponential factors $\ln A_i$ and the exponential coefficients B_i printed by the Lat-PC program for the system C_2H_6/CaO

	Values	Standard errors	r^2
$\ln A_1$	12.61	±0.03	0.999
$\ln A_2$	13.4	±0.9	
$\ln A_3$	13.086	±0.010	
$\ln A_4$	12.88	±0.04	
$\ln A_5$	12.656	±0.005	0.999
$\ln A_6$	12.3	±0.6	
$\ln A_7$	12.32	±0.11	
B_1	−0.01872	$\pm 2.4 \times 10^{-4}$	0.999
B_2	-8.6×10^{-2}	$\pm 1.0 \times 10^{-2}$	
B_3	-7.232×10^{-2}	$\pm 2.5 \times 10^{-4}$	
B_4	−0.3826	$\pm 4 \times 10^{-3}$	
B_5	-1.909×10^{-2}	$\pm 5 \times 10^{-5}$	0.999
B_6	−0.162	$\pm 2.2 \times 10^{-2}$	
B_7	−0.276	$\pm 1.5 \times 10^{-2}$	

In conclusion, all plots in parts (b) and (c) of Figs. 1 and 3 show three kinds of active sites for adsorption in all five systems: C_2H_6/CaO, C_2H_4/CaO, C_2H_2/CaO, C_3H_6/CaO, and 1-C_4H_8/CaO, as in a previous publication [25] concerning the adsorption characterization of MgO under similar conditions.

In all five systems: C_2H_2/CaO, C_2H_4/CaO, C_2H_6/CaO, C_3H_6/CaO, and 1-C_4H_8/CaO, the following can be noticed, from left to right: (a) the shape of the curves remains almost unchanged; (b) a displacement of the maxima concerning the energy distribution function to higher time values under the same experimental conditions; (c) an increase of the area under the third curve. Thus, all five systems show about the same adsorption behavior.

As regards parts (a) and (b) of Figs. 2 and 4, the hydrocarbon molecules at time t are not assumed to be adsorbed on sites of the same energy as in [22,24] concerning other adsorbents. The maxima and minima represent again transition adsorption energies in all these cases.

From Table 1 and Figs. 2 and 4 (part c), it is seen the time dependence of c^*_{max} and c_y as one can expect from Eqs. (2) to (5). On the other hand, the adsorbed

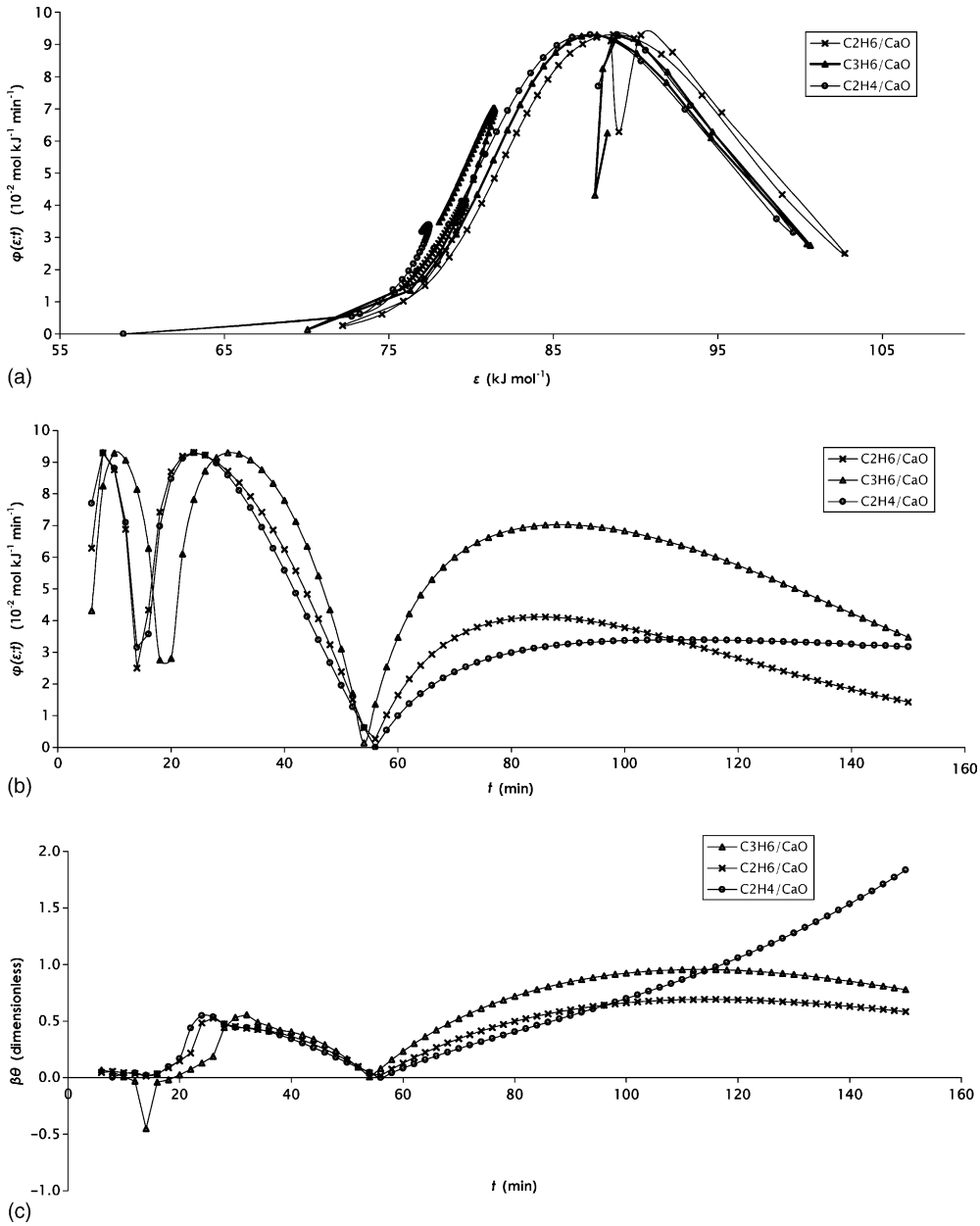

Fig. 1. Plots of : (a) distribution function $\phi(\varepsilon; t)$ against adsorption energy values ε, (b) distribution function $\phi(\varepsilon; t)$ as a function of time, and (c) the lateral molecular interaction energy $\beta\theta_i$ (dimensionless) as a function of time for C_2H_6, C_2H_4, and C_3H_6 on CaO at 323.2 K.

amount c_s^* is not a unique function of the gas phase concentration c_y, as expected from an ordinary and conventional adsorption isotherm [1]. It seems that a single partial pressure corresponding to $c_{y,}$ can produce two different surface coverages at some areas. This behavior stems from the fact that Eq. (3) does not give the total monolayer coverage of the entire homogeneous surface, but it is a local adsorption equation for a heterogeneous surface, sweeping it over the various active sites of different adsorption energy with

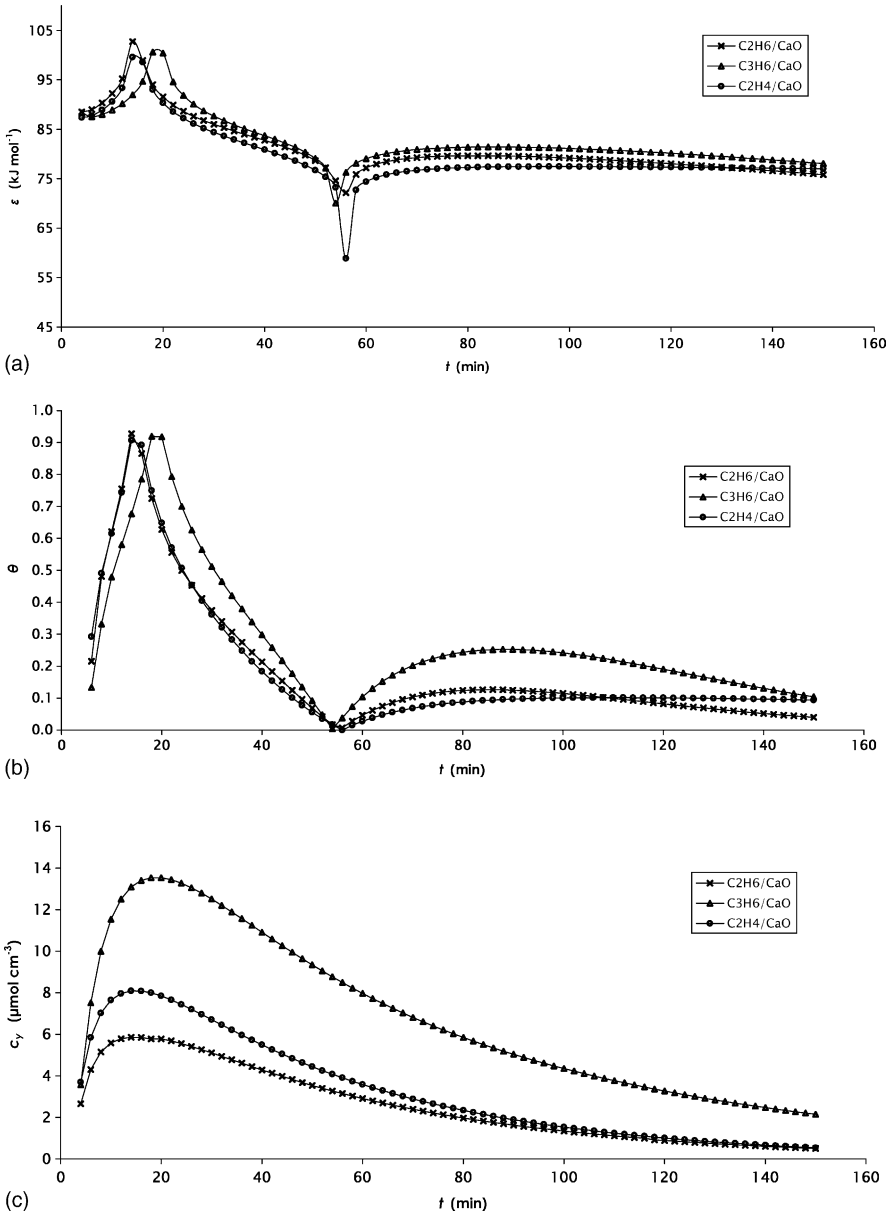

Fig. 2. Plots of : (a) local adsorption energy ε, (b) local adsorption isotherm θ_i, and (c) gaseous adsorbate concentration c_y, as a function of time for C_2H_6, C_2H_4, and C_3H_6 on CaO at 323.2 K.

time. It is an usual experimental finding for c_y to increase with time initially, reach a maximum and then decrease exponentially with time, as one can see for all the systems in Figs. 2 and 4 (part c). Two different time periods may exhibit the same value for $c_{y,}$ one in the ascending branch and the other in the descending one. But these do not correspond to the same value for the adsorbed concentration c_s^*, since different kinds of adsorption sites contribute to the adsorption process in the above two cases, i.e. at two different times [1].

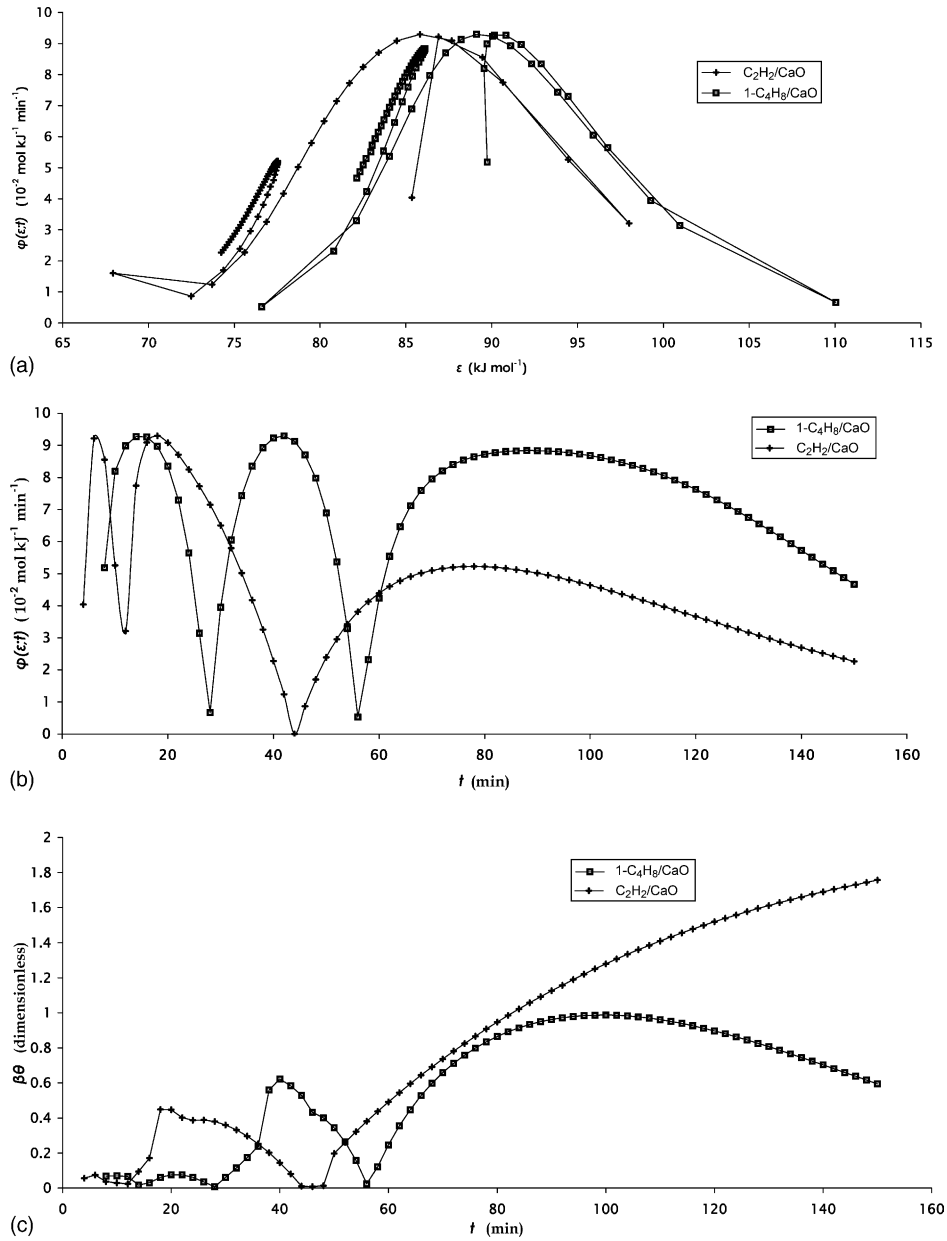

Fig. 3. Plots of : (a) distribution function $\phi(\varepsilon; t)$ against adsorption energy values ε, (b) distribution function $\phi(\varepsilon; t)$ as a function of time, and (c) the lateral molecular interaction energy $\beta\theta_i$ (dimensionless), as a function of time for C_2H_2, and C_4H_8 on CaO at 323.2 K.

The maximum value for c_y corresponding to a certain c_s^* may be due to a completion of a monolayer of adsorbed molecules. Further increase of c_s^* can be interpreted as due to multilayer adsorption, causing a decrease in c_y [11].

4.1. Comparison with other methods

Adsorption isotherms and surface energy distribution functions on heterogeneous surfaces have been the subject of many efforts during the last two decades for

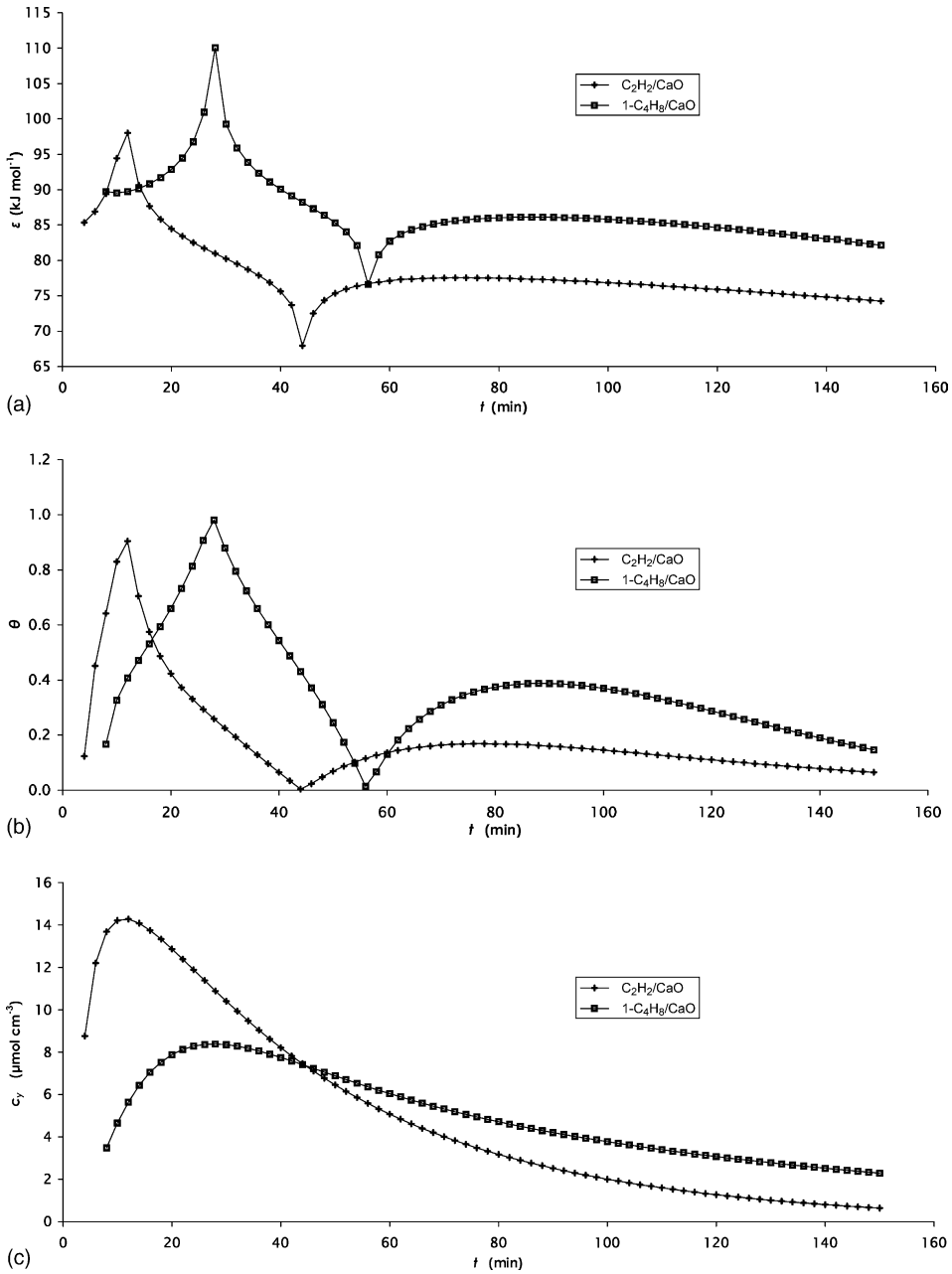

Fig. 4. Plots of : (a) local adsorption energy ε, (b) local adsorption isotherm θ_i, and (c) gaseous adsorbate concentration c_y, as a function of time for C_2H_2 and C_4H_8 on CaO at 323.2 K.

characterizing heterogeneous solids by calculating adsorption energy distribution functions from retention volume data. All these works offer approximate functions or values through approximate solutions without any determination of the actual values of adsorption parameters [5,24–26].

Of all the classical methods for measuring adsorption energies, isotherms etc. none has led to local

values. These methods lack the precision and the possibility of the RF-GC method. Difficulties like these led scientists to turn into numerical solutions [1–4,27–30].

The RF-GC method has the following advantages [1,11]: (1) it is simple and fast; (2) it is accurate; (3) the diffusion and resistance to mass transfer are taken into account while pressure gradient along the bed is negligible; (4) it leads directly to experimental isotherm without specifying an isotherm equation a priori; and (5) the isotherm can be determined in the presence of a surface reaction of the adsorbate.

Beyond that, it creates a domain of time-resolved chemistry of surfaces which provides experimental local values of adsorption energies, adsorption isotherms, monolayer capacities, probability density functions, and lateral molecular interactions. Thus, all physicochemical quantities mentioned above can be determined as functions of experimental time by means of a simple PC program, the LAT one [26]and the plots can be provided through an Excel PC program.

5. Conclusions

In this work, the adsorption of many significant hydrocarbons is investigated. The adsorbent in this study was calcium oxide. Thus, a systematic study of five heterogeneous systems C_XH_Y/CaO and their characterization through some new physicochemical parameters is presented. The technique used is the RF-GC, a version of inverse chromatography which has the stationary phase of the heterogeneous system as its object of investigation. Determination of these new physicochemical parameters on well-characterized adsorbents will provide the data base needed for the development of models by which analyze and interpret such data.

Acknowledgements

The authors acknowledge the financial support from the National Technical University of Athens under the research program THALIS 2002-2003.

References

[1] F. Roubani-Kalantzopoulou, J. Chromatogr. A 806 (1998) 293.
[2] M. Domingo-Garcia, F.J. Lopez-Garzon, R. Lopez-Garzon, C. Moreno-Castilla, J. Chromatogr. 324 (1985) 19.
[3] J. Jaroniec, Phys. Lett. 59A (4) (1976) 259.
[4] J. Roles, G. Guiochon, J. Chromatogr. 591 (1992) 233.
[5] M. Jaroniec, R. Madey, Physical Adsorption on Heterogeneous Solids, Elsevier, Oxford, New York, 1988.
[6] N.A. Katsanos, Flow Pertubation Gas Chromatography, Dekker (Marcel), New York, Basel, 1988.
[7] N.A. Katsanos, R. Thede, F. Roubani-Kalantzopoulou, J. Chromatogr. A 795 (1998) 133.
[8] H. Metaxa, E. Kalogirou, F. Roubani-Kalantzopoulou, Russian J. Phys. Chem. 73 (1999) 112.
[9] A. Kalantzopoulos, Ch. Abatzoglou, F. Roubani-Kalantzopoulou, Colloids Surf. A 151 (1999) 377.
[10] E. Kalogirou, I. Bassiotis, Th. Artemiadi, S. Margariti, V. Siokos, F. Roubani-Kalantzopoulou, J. Chromatogr. A 969 (2002) 81.
[11] V. Sotiropoulou, G.P. Vassilev, N.A. Katsanos, H. Metaxa, F. Roubani-Kalantzopoulou, J. Chem. Soc., Faraday Trans. 91 (1995) 485.
[12] V. Sotiropoulou, N.A. Katsanos, H. Metaxa, F. Roubani-Kalantzopoulou, Chromatographia 42 (1996) 441.
[13] F. Roubani-Kalantzopoulou, E. Kalogirou, A. Kalantzopoulos, H. Metaxa, R. Thede, N.A. Katsanos, V. Sotiropoulou, Chromatographia 46 (1997) 161.
[14] X. Yun, Z. Long, D. Kou, X. Lu, H. Li, J. Chromatogr. A 736 (1996) 151.
[15] Ch. Abatzoglou, E. Iliopoulou, N.A. Katsanos, F. Roubani-Kalantzopoulou, A. Kalantzopoulos, J. Chromatogr. A 775 (1997) 211.
[16] H. Zahariou-Rakanta, A. Kalantzopoulos, F. Roubani-Kalantzopoulou, J. Chromatogr. A 776 (1997) 275.
[17] G. Karagiorgos, F. Roubani-Kalantzopoulou, Z. Phys. Chem 203 (1998) 231.
[18] S. Birbatakou, I. Pagopoulou, A. Kalantzopoulos, F. Roubani-Kalantzopoulou, J. Chim. Phys. 95 (1998) 2180.
[19] D. Gavril, A. Koliadima, G. Karaiskakis, Langmuir 15 (1999) 3798.
[20] D. Gavril, G. Karaiskakis, J. Chromatogr. A 845 (1999) 67.
[21] N.A. Katsanos, N. Rakintzis, F. Roubani-Kalantzopoulou, E. Arvanitopoulou, A. Kalantzopoulos, J. Chromatogr. A 845 (1999) 103.
[22] N.A. Katsanos, E. Arvanitopoulou, A. Kalantzopoulos, F. Roubani-Kalantzopoulou, J. Phys. Chem. B 103 (1999) 1152.
[23] N.A. Katsanos, F. Roubani-Kalantzopoulou, Adv. Chromatogr. 40 (2000) 231.
[24] N.A. Katsanos, E. Iliopoulou, F. Roubani-Kalantzopoulou, E. Kalogirou, J. Phys. Chem. B 103 (1999) 10228.
[25] F. Roubani-Kalantzopoulou, Th. Artemiadi, I. Bassiotis, N.A. Katsanos, V. Plagianakos, Chromatographia 53 (2001) 315.

[26] N.A. Katsanos, F. Roubani-Kalantzopoulou, E. Iliopoulou, I. Bassiotis, V. Siokos, M.N. Vrahatis, V.P. Plagianakos, Colloids Surf. A 201 (2002) 173.
[27] T. Paryjczak, Gas Chromatography in Adsorption and Catalysis, Ellis Horwood, Chichester, 1986.
[28] W. Rudzinski, D. H.Everett, Adsorption of Gases on Heterogeneous Surfaces, Academic Press, New York, 1992.
[29] B.J. Stanley, G. Guiochon, J. Phys. Chem. 97 (1993) 8098.
[30] M. Heuchel, M. Jaroniec, R.K. Gilpin, J. Chromatogr. 628 (1993) 59.